



Fluences of solar energetic particles for last three GLE events: Comparison of different reconstruction methods

Sergey Koldobskiy^{a,b,c,*}, Alexander Mishev^{a,b}

^a *Sodankylä Geophysical Observatory, University of Oulu, Oulu, Finland*

^b *Space Physics and Astronomy Research Unit, University of Oulu, Oulu, Finland*

^c *National Research Nuclear University MEPhI, Moscow, Russia*

Received 13 August 2021; accepted 26 November 2021

Abstract

Fluxes of solar energetic particles (SEPs), produced and accelerated in and in the vicinity of the Sun, are an important part of cosmic ray induced terrestrial effects such as ionizing radiation on the Earth's orbit, which affects the exposure to radiation in space as well as the atmospheric ionization. Calculation of these effects requires the knowledge of the integral fluences of SEPs. High-energy solar particles are subject of special interest since they can significantly contribute to the total radiation dose and/or ionization. The main instrument to study the high-energy SEP events is a network of ground-based neutron monitors (NMs), used over the years to register a specific class of SEP, which is called ground-level enhancement (GLE) events. Up today, we possess records from 72 GLE events. Reconstruction of SEP integral and differential fluxes for GLE events using NM data is not an easy task, requires a careful and precise calculation of particle transport in the magnetosphere, atmosphere, and detector itself. In this work, we compare two methods of fluence reconstruction, "fast" and "full", for the last three registered GLE events and additionally verify one of them using PAMELA experimental data.

© 2022 COSPAR. Published by Elsevier B.V. This is an open access article under the CC BY license (<http://creativecommons.org/licenses/by/4.0/>).

Keywords: Solar energetic particle; Ground level enhancement; Neutron monitor

1. Introduction

High-energy charged particles, such as galactic cosmic rays (GCRs) and solar energetic particles (SEPs), play an important role in the processes of the Earth's atmosphere, specifically in precipitating particles induced ionization and determine the complex radiation field at flight altitudes. Therefore, the careful consideration of their fluxes is crucial for understanding the ionization processes and assessment of ionization doses for aircraft crew and passengers, manned and unmanned missions in the vicinity of the

Earth (e.g. [Mironova et al., 2015](#); [Vainio et al., 2009](#), and references therein).

Fluxes of galactic cosmic rays are presented (in the number of particles) mainly by protons (~90%) and α -particles (~8%) and a small amount of heavier-than-helium nuclei, positrons, and electrons. Differential fluxes of cosmic ray-particles are well-known today, thanks to pioneering results of PAMELA ([Adriani et al., 2017](#)) and AMS-02 space experiments ([Aguilar et al., 2021](#)). GCR fluxes are influenced by the solar modulation ([Potgieter, 2013](#)) and are time-dependent. They anti-correlate with the level of the solar activity, being less intense during the solar maxima, accordingly more intense during the solar minima. The modulation process is energy-dependent, so that fluxes of low-energy particles can differ up to ~10 times during the maxima and minima, while the effect is marginal for

* Corresponding author.

E-mail addresses: sergey.koldobskiy@oulu.fi (S. Koldobskiy), alexander.mishev@oulu.fi (A. Mishev).

particles with energies ≥ 30 GeV/n. Detailed study of the solar modulation process (e.g., the charge-sign dependence of the modulation) requires the opportunity to separately measure fluxes of different cosmic-ray species, and it is possible only for the last decade using PAMELA and AMS-02 data.

The study of GCRs modulation on extended timescales is possible by using records from the worldwide neutron monitor (NM) network. NMs are energy-integrating detectors, which can register mainly the hadron component of secondary particle showers, produced during the interaction of primary cosmic ray particles with the atmospheric nuclei. The global NM network was developed in the mid-1950s, nowadays it is used for different purposes (e.g. Mavromichalaki et al., 2011, 2018; Miroshnichenko, 2018). Since NMs are located in different geomagnetic cut-off rigidities, they can be used as a giant spectrometer, so that it is possible to estimate the level of solar activity using a simplified one-parameter model, that is the force-field model (Gleeson and Axford, 1968). This model is very useful for quantifying the solar activity and it is appropriate for different applications (e.g. Usoskin, 2017). Besides, the global NM network is used for the systematic study of SEPs.

Solar energetic particles (mainly consisting of protons) are accelerated in and in the vicinity of the Sun during solar eruptive events, such as solar flares and coronal mass ejections (CMEs), and can be additionally accelerated during their propagation in the heliosphere. Solar flares and CMEs occur with greater probability in periods of increased solar activity. Low-energy SEPs can be registered by satellite experiments, such as GOES (energy range $10 \leq E(\text{MeV}) \leq 500$, see an example in Raukunen et al., 2020). Both low- and high-energy particles were registered by the PAMELA experiment ($E > 100$ MeV, Bruno et al., 2018) and are observed by the AMS-02 experiment (results are not yet published), however, these measurements are available only for the period 2006 onward. Higher-energy SEPs can be registered by NMs if they are energetic enough to initiate atmospheric shower, whose secondaries can reach the Earth's surface. Such type of SEP events is called ground-level enhancements (GLEs, see, e.g. Poluianov et al., 2017). At present, 72 GLE events are known, the first four were registered during the pre-NM era using ionization chambers and currently there are no reliable data for these events. GLEs starting from #5 were registered by NMs and their records are stored in the International GLE Database (IGLED, see Usoskin et al., 2020, for details), which give the basis for their analysis.

Reconstruction of SEP fluxes (both differential and integral, the latter called fluence) using the NM data is not an easy task. In particular, it is necessary to understand the high-energy cosmic-ray propagation in the magnetosphere and atmosphere of the Earth (e.g. Mishev and Usoskin, 2020, and references therein), as well as their interactions

with the detector itself. A convenient approach is the employment of the NM yield function (YF), widely used in the NM community. NM YF allows one to calculate the device count rate by knowing the spectra of primary cosmic ray particles.

Several YFs were recently calculated using Monte-Carlo event generators and/or NM latitude surveys (e.g. Caballero-Lopez and Moraal, 2012; Mangeard et al., 2016; Nuntiyakul et al., 2018). Recently, AMS-02 observations (Aguilar et al., 2018) allowed us to verify different YFs (Koldobskiy et al., 2019a) and the best performance was shown by the YF calculated by Mishev et al., 2013, which was updated and expanded to different atmospheric depths (Mishev et al., 2020). Secondly, the analysis itself requires considering a lot of features. In a more simplified approach (Koldobskiy et al., 2018, 2019b, 2021; Usoskin et al., 2020) neutron monitors are considered as energy-integrating detectors and for each NM the value of energy and corresponding scale factor between the SEP-induced signal and the particle fluence is calculated. This approach did not consider the anisotropy of SEPs and their temporal variability. However, these simplifications allowed to scale the method of integral flux reconstruction for 58 strongest GLE events. After that, high-energy SEP fluxes were combined with low-energy data from GOES satellites, the PAMELA experiment, and other measurements before 1989 to get the integral fluxes for energies > 30 MeV. Another approach (see examples in, e.g., Mishev et al., 2021a,b) considers the temporal variability of the fluxes and their anisotropy and allows to reconstruct (in addition to integral fluxes) also the variability of differential fluxes and their pitch-angle distributions (PADs). However, this approach requires extensive computations, it is time-consuming and considers careful modeling of the geomagnetic conditions, which differs for each GLE event.

Since for practical applications, such as atmospheric ionization and calculation of the radiation dose in the vicinity of the Earth or flight altitudes (e.g. Vainio et al., 2009), as well as to quantify the energy budget of SEPs in relation to their acceleration mechanism(s) (e.g. Kocharov et al., 2018, 2020, 2021), the integral fluence is used as an input and/or as an important part of the corresponding model (s), it is important to compare the results of integral fluence reconstruction using both approaches and use satellite data (if available) to cross-check this result. In this work, we compare the results for the fluence reconstruction using both (full and fast) approaches for the last three GLE events, which encompass almost all possible angular distribution of SEPs.

2. Analysis and results

2.1. Full analysis of GLEs using NM data

In general, it is possible to derive the spectral and angular characteristics of nearly relativistic and relativistic SEPs using NM records of GLEs (e.g. Shea and Smart, 1982).

Normally, it is performed by modeling the global NM response and subsequent inverse problem solution, that is an optimization of a set of model parameters over the experimental data points. Here, the modeling of the NM network is made using the relationship between the NM count rates and the primary cosmic-ray flux, i.e., using recently computed NM yield function (Mishev et al., 2013, 2020). The latter is experimentally verified with latitude surveys and direct space-borne measurements of GCRs by PAMELA (Payload for Antimatter Matter Exploration and Light-nuclei Astrophysics, Adriani et al., 2017) and AMS-02 (Alpha Magnetic Spectrometer, Aguilar et al., 2021), for details see Mishev et al. (2013), Gil et al. (2015), Mangeard et al. (2016), Nuntiyakul et al. (2018), Koldobskiy et al. (2019a). The most important, we modeled the response of each NM using a specific yield function corresponding to the exact station altitude above sea level (for details see Mishev et al., 2018, 2020, 2021a). This allowed us to reduce unfolding procedure uncertainties due to the employment of the double-attenuation-lengths method (e.g. McCracken et al., 1962).

In the model different approximations of SEP spectra can be assumed, such as a modified power-law rigidity spectrum similarly to Cramp et al. (1997), Vashenyuk et al. (2006):

$$J(P) = J_0 P^{-(\gamma + \delta\gamma(P-1))} \quad (1)$$

where $J(P)$ is the particle flux as a function of rigidity P in GV, γ is the power-law spectral exponent at rigidity $P = 1$ GV, accordingly, $\delta\gamma$ is the rate of the spectrum steepening; or an exponential spectrum:

$$J(P) = J_0 \exp(-P/P_0). \quad (2)$$

where $J(P)$ is defined in the same way as in Eq. 1, accordingly P_0 is a characteristic proton rigidity.

In the model, the PAD can be approximated with a complicated distribution, that is, double (Sun-anti Sun) Gaussian:

$$G(\alpha(P)) \sim \exp(-\alpha^2/\sigma_1^2) + B \cdot \exp(-(\alpha - \pi)^2/\sigma_2^2) \quad (3)$$

where α is the pitch angle, σ_1 and σ_2 are parameters governing the width of the distribution, B accounts for the contribution of the particles arriving from the anti-Sun direction. When $B = 0$, the PAD is simplified to a Gaussian distribution along the axis of the apparent source direction. Therefore, we can model simple PAD of GLE particles ($B = 0$) and complicated angular distributions, including particle flux from the anti-Sun direction.

Here, the inversion of the spectra and PAD of SEPs was performed using a method based on Levenberg–Marquardt numerical approach (Levenberg, 1944; Marquardt, 1963) employing flexible regularization (for details see Aleksandrov, 1971; Golub and Van Loan, 1980; Golub et al., 1999), which allows one to solve the ill-posed problem(s), frequently arising from marginal experimental NM responses and/or complicated spectral and angular distribution(s), e.g. bi-directional flux of SEPs shapes (see

the discussions in Tikhonov et al., 1995; Mavrodiev et al., 2004; Aster et al., 2005; Mishev et al., 2017, 2018). This specific method was recently verified with PAMELA space probe direct observations, see the text below for GLE #71.

2.2. Fast analysis of GLEs using NM data

The method of the fast NM analysis allows to reconstruct only the SEP fluence using the integral GLE signals by different NMs, it was gradually developed in Koldobskiy et al., 2018, 2019b. In this approach, each NM considered an energy and time-integrating detector of the SEPs and characterized by two values: the effective rigidity R and corresponding scale factor κ which allows calculating the fluence of SEPs using the following equation:

$$F(> R) = \kappa \cdot N_{GLE} \quad (4)$$

where N_{GLE} is an integral count rate of NM due to SEP particles.

This approach does not consider the anisotropy of SEP fluxes and their evolution in time, however, for the most part of GLE events we have at least about 15–20 NMs which registered the signal so that it is possible to reconstruct the averaged fluence during the event. After reconstruction of fluence points (one point per one NM for each GLE event), the rigidity dependence was fitted with power-law exponential decay function (Usoskin et al., 2020). In Koldobskiy et al., 2021 the low-energy SEP measurements from different missions were also added to the analysis and obtained fluences in the wide energy range from ~ 30 MeV to ~ 10 GeV were fitted with modified Band function. Here we use the results of this latest reconstruction.

2.3. Results

2.3.1. GLE #70

GLE #70 occurred on 13 December 2006, during the declining phase of the solar cycle 23. The GLE signal was registered by 31 NMs, highest-rigidity NM registered the signal was HRMS ($P_c = 4.43$ GV, $N = 1.5\% \cdot \text{hour}$, where N is an integral GLE increase) and the maximum GLE signal was observed in OULU NM ($N = 103\% \cdot \text{hour}$). The event occurred during the lifetime of the PAMELA experiment, however, the SEP fluence reconstruction for that event is restricted to the second half of the event that does not reflect the full-event SEP fluence. Yet, the full modeling has been performed by several teams, here we provide the derived SEP spectra by Mishev and Usoskin, 2016a,b, presented in Fig. 1. Similar to some other events it was characterized by a large anisotropy in its initial phase (Bütikofer et al., 2009; Vashenyuk et al., 2008), where a beam-like SEP flux was revealed. In addition, during the event onset, SEPs possessed hard spectra, however gradual softening was observed throughout the event. Besides, a relatively fast isotropization was observed after the initial

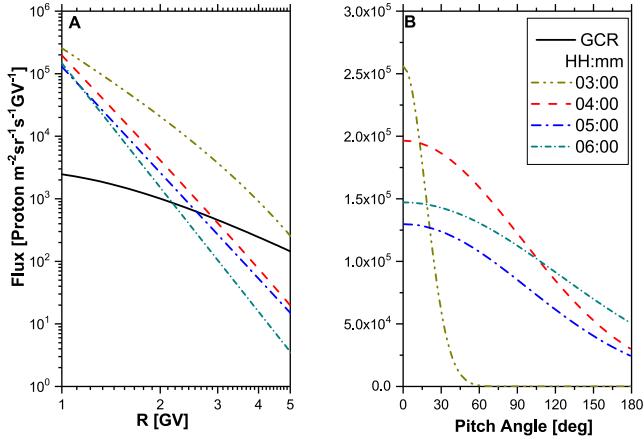


Fig. 1. Derived proton spectra and PAD during GLE #70 using full NM modelling. The left-hand (A) panel depicts the SEP spectra, where the black solid line corresponds to the GCRs, while the right-hand (B) corresponds to PAD. The characteristics are shown for several stages of the event as depicted in the legend.

phase of the event. Therefore, assuming an isotropic SEP flux for the computation of the fluence using the fast method is a reasonable approach.

Using the derived SEP spectra and PAD employing the full NM data analysis and the simplified fast analysis, we computed the angle-, energy-, and time-integrated fluence. Very good agreement of the derived fluence during GLE #70 between the full and fast method of analysis was achieved, the details are presented in Fig. 2. The presented in Fig. 2 confidence limits encompass the uncertainties due to the method itself, as well as those related to the new NM yield function.

2.3.2. GLE #71

GLE #71 took place on 17 May 2012, during the inclining phase of the solar cycle 24. The GLE signal was regis-

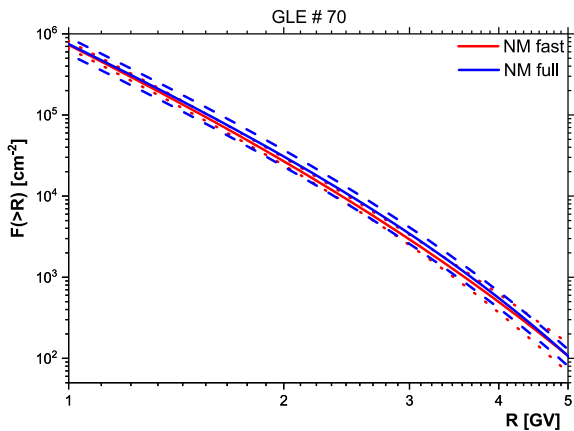


Fig. 2. Angle-, energy-, and time-integrated SEP fluence during GLE #70 derived with full and fast NM modelling as depicted in the legend. The dash and dot lines determine the 95% confidence limit for full and fast analysis, respectively.

tered by 16 NMs, highest-rigidity NM registered the signal was KIEL ($P_c=2.25$ GV, $N = 1\%*$ hour) and the maximum GLE signal was observed in SOPO NM ($N = 17\%*$ hour). The corresponding SEP event was also detected by the PAMELA experiment and its integral fluence was reconstructed, accordingly. The derived SEP spectra and PAD at selected stages of the event using the full modeling are presented in Fig. 3, the details are given elsewhere (Mishev et al., 2021b). We note, during the event onset and initial phase a complicated PAD was derived, namely approximated with double Gaussian (Fig. 3, the top right panel). Accordingly, during the initial phase (01:50–02:25 UT) a relatively hard spectrum, described with modified power-law, with gradual increase of SEP flux was derived, yet a steady softening of the SEP spectra and decrease of the SEP flux were observed during the main and late phase of the event (after 03:05 UT). However, the event-averaged spectrum was relatively soft with marginal steepening, accordingly, the PAD was relatively broad with marginal anisotropy. Therefore, the assumption of isotropic SEP flux employed for the fast method for analysis is reasonable.

The computed fluence using the full and fast method is presented in Fig. 4. Besides, a very good agreement of the derived fluence during GLE #71 with the direct measurements made by PAMELA space-probe was achieved (Bruno et al., 2018), the details are given in Koldobskiy et al., 2019b. Here, we would like to stress that PAMELA detectors allowed one measure of SEPs for rigidities less than about 2 GV. Moreover, the direct measurements with PAMELA and ERNE revealed a similar complicated angular distribution of SEPs (e.g., Adriani et al., 2015), while the integral spectra were fitted with Ellison–Ramaty spectral form (e.g. Ellison and Ramaty, 1985).

One can see the very good agreement of both full and fast methods with the direct space-borne measurements.

2.3.3. GLE #72

GLE #72 have been registered on 10 September 2017, during the declining phase of the solar cycle 24. The GLE signal was registered by 17 NMs, the highest-rigidity NM registered the signal was LMKS ($P_c=3.69$ GV) and the maximum GLE signal was observed in TERA ($N = 38\%*$ hour). The GLE onset was observed at about 16:15 UT (e.g. by FSMT and INVK NMs). However, a statistically significant signal, which allowed us to derive the spectra and PAD of the SEPs with reasonable precision, was observed at 16:30 UT.

Here, the best fit was obtained assuming a modified power-law rigidity spectrum of SEPs and double Gaussian PAD, that is we revealed particles arriving from Sun and anti-Sun direction, the details are given elsewhere (Mishev et al., 2018; Mishev and Usoskin, 2018). In general, the derived PAD, specifically after the main phase of the event, was broad enough, so that the assumption of isotropic SEP flux employed in fast data analysis can be reasonably applied.

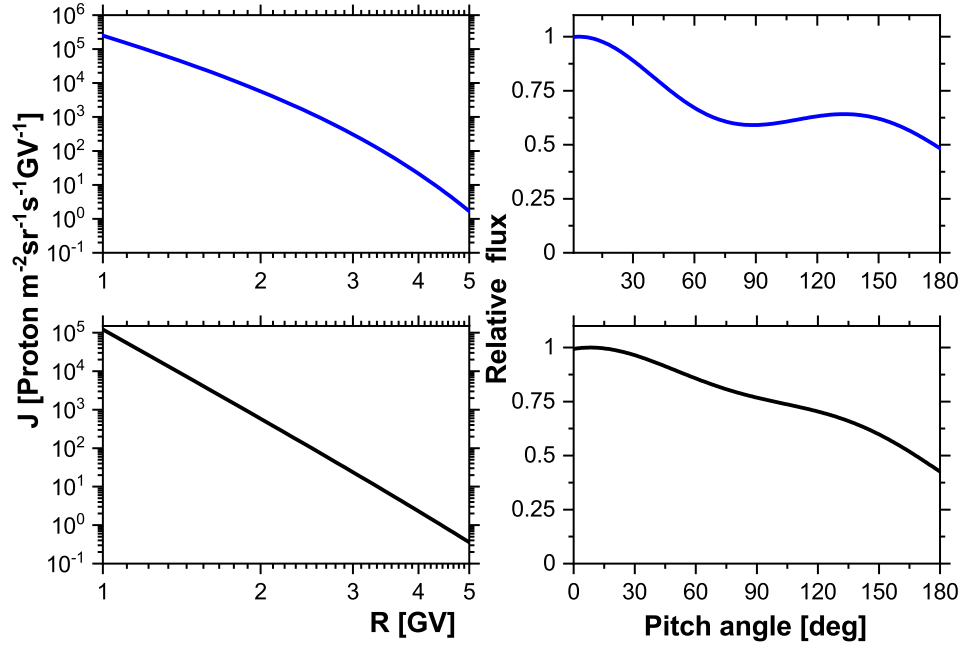


Fig. 3. The same as Fig. 1, but for GLE #71. The top panels correspond to the initial phase of the event 01:50 UT–02:25 UT, the lower panels correspond to the average over the whole event.

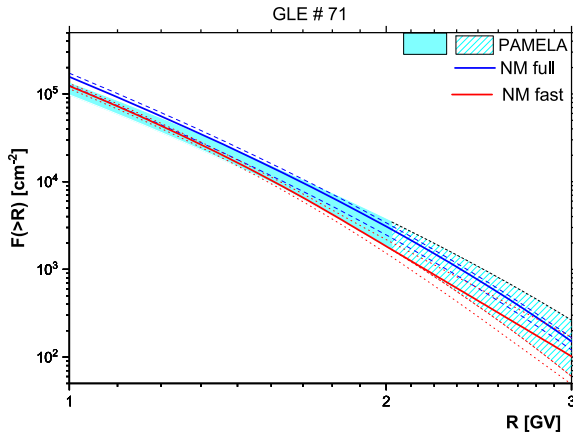


Fig. 4. The same as Fig. 2, but for GLE #71. In addition, direct measurements of PAMELA experiment (with uncertainties) are shown with the blue filled area. The filled and hatched area correspond to the PAMELA data up to 2 GV and data extrapolation above 2 GV respectively.

Similar to the previous two cases, we computed the particle fluence during GLE #72, presented in Fig. 5. One can see the good agreement between the two methods.

3. Discussion and conclusions

In this work, we reconstructed the spectral and angular characteristics of GLE particles during several events, namely the last three observed by the global NM network. On the basis of the obtained spectra, we derived the energy-, angular-, and time-integrated fluence of SEPs during the considered events using two different approaches as described in Section 2. We studied events with different

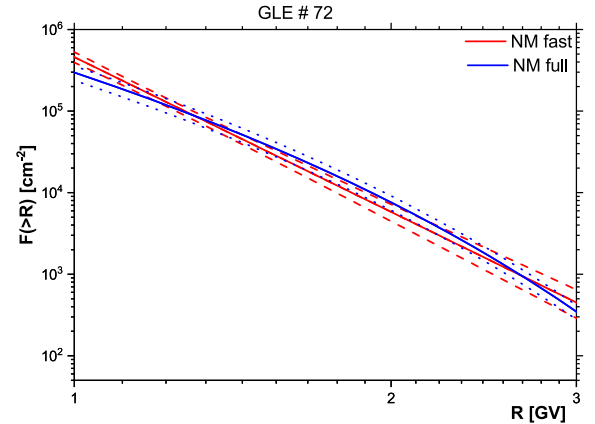


Fig. 5. The same as Fig. 2, but for GLE #72.

PADs, a simple Gaussian-like (GLE #70), complicated shifted double Gaussian (GLE #71), and Sun anti-Sun double SEP flux (GLE #72). The selected GLEs encompass almost all possible cases of angular distributions of GLE particles. Besides, one of the events was observed by a space-borne experiment, which allowed us to compare direct and ground-based measurements and the corresponding results from the analysis. In addition, we explicitly assessed the uncertainty and confidence limits of the derived fluence.

A good agreement between the different approaches is achieved. Therefore, the fast method for estimation of the SEP fluence during moderately strong and weak GLEs, even with complicated PAD, is a reasonable approach and can be employed for different purposes related to the quantification of cosmic-ray terrestrial effects.

Declaration of Competing Interest

The authors declare that they have no known competing financial interests or personal relationships that could have appeared to influence the work reported in this paper.

Acknowledgments

This work was supported by the Academy of Finland (projects 330064 QUASARE, 321882 ESPERA) and by the Russian Science Foundation project No. 20-72-10170 (in part of the fast method of SEP fluence reconstruction). The work was motivated and benefited from discussions in the framework of the International Space Science Institute International Team 441: High EneRgy sOLar partICle Events Analysis (HEROIC).

References

- Adriani, O., Barbarino, G.C., Bazilevskaya, G.A., Bellotti, R., Boezio, M., Bogomolov, E.A., Bongì, M., Bonvicini, V., Bottai, S., Bravar, U., Bruno, A., Cafagna, F., Campana, D., Carbone, R., Carlson, P., Casolino, M., Castellini, G., Christian, E.R., Donato, C.D., de Nolfo, G.A., Santis, C.D., Simone, N.D., Felice, V.D., Formato, V., Galper, A.M., Karelin, A.V., Koldashov, S.V., Koldobskiy, S., Krutkov, S.Y., Kvashnin, A.N., Lee, M., Leonov, A., Malakhov, V., Marcelli, L., Martucci, M., Mayorov, A.G., Menn, W., Mergè, M., Mikhailov, V. V., Mocchiutti, E., Monaco, A., Mori, N., Munini, R., Osteria, G., Palma, F., Panico, B., Papini, P., Pearce, M., Picozza, P., Ricci, M., Ricciarini, S.B., Ryan, J.M., Sarkar, R., Scotti, V., Simon, M., Sparvoli, R., Spillantini, P., Stochaj, S., Stozhkov, Y.I., Thakur, N., Vacchi, A., Vannuccini, E., Vasilyev, G.I., Voronov, S.A., Yurkin, Y. T., Zampa, G., Zampa, N., 2015. PAMELA's measurements of magnetospheric effects on high-energy solar particles. *Astrophys. J.* 801 (1), L3. <https://doi.org/10.1088/2041-8205/801/1/L3>.
- Adriani, O., Barbarino, G.C., Bazilevskaya, G.A., Bellotti, R., Boezio, M., Bogomolov, E.A., Bongì, M., Bonvicini, V., Bottai, S., Bruno, A., Cafagna, F., Campana, D., Carlson, P., Casolino, M., Castellini, G., De Santis, C., Di Felice, V., Galper, A.M., Karelin, A.V., Koldashov, S.V., Koldobskiy, S., Krutkov, S.Y., Kvashnin, A.N., Leonov, A., Malakhov, V., Marcelli, L., Martucci, M., Mayorov, A.G., Menn, W., Mergè, M., Mikhailov, V.V., Mocchiutti, E., Monaco, A., Munini, R., Mori, N., Osteria, G., Panico, B., Papini, P., Pearce, M., Picozza, P., Ricci, M., Ricciarini, S.B., Simon, M., Sparvoli, R., Spillantini, P., Stozhkov, Y.I., Vacchi, A., Vannuccini, E., Vasilyev, G., Voronov, S. A., Yurkin, Y.T., Zampa, G., Zampa, N., 2017. Ten Years of PAMELA in Space. *Rivista del Nuovo Cimento*, 40(10), 473–522. <https://doi.org/10.1393/ncr/i2017-10140-x>, URL: <http://arxiv.org/abs/1801.10310>, <https://doi.org/10.1393/ncr/i2017-10140-x>.
- Aguilar, M., Ali Cavazonza, L., Alpat, B., Ambrosi, G., Arruda, L., Attig, N., Aupetit, S., Azzarello, P., Bachlechner, A., Barao, F., Barrau, A., Barrin, L., Bartoloni, A., Basara, L., Başeğmez-du Pree, S., Battarbee, M., Battiston, R., Becker, U., Behlmann, M., Beischer, B., Berdugo, J., Bertucci, B., Bindel, K.F., Bindi, V., de Boer, W., Bollweg, K., Bonnivard, V., Borgia, B., Boschini, M.J., Bourquin, M., Bueno, E.F., Burger, J., Cadoux, F., Cai, X.D., Capell, M., Caroff, S., Casaus, J., Castellini, G., Cervelli, F., Chae, M.J., Chang, Y.H., Chen, A.I., Chen, G.M., Chen, H.S., Chen, Y., Cheng, L., Chou, H.Y., Choumilov, E., Choutko, V., Chung, C.H., Clark, C., Clavero, R., Coignet, G., Consolandi, C., Contin, A., Corti, C., Creus, W., Crispoltoni, M., Cui, Z., Dadzie, K., Dai, Y.M., Datta, A., Delgado, C., Della Torre, S., Demirköz, M.B., Derome, L., Di Falco, S., Dimiccoli, F., Díaz, C., von Doetinchem, P., Dong, F., Donnini, F., Duranti, M., D'Urso, D., Egorov, A., Eline, A., Eronen, T., Feng, J., Fiandrini, E., Fisher, P., Formato, V., Galaktionov, Y., Gallucci, G., García-López, R.J., Gargiulo, C., Gast, H., Gebauer, I., Gervasi, M., Ghelfi, A., Giovacchini, F., Gómez-Coral, D.M., Gong, J., Goy, C., Grabski, V., Grandi, D., Graziani, M., Guo, K.H., Haino, S., Han, K.C. et al. (2018). Observation of Fine Time Structures in the Cosmic Proton and Helium Fluxes with the Alpha Magnetic Spectrometer on the International Space Station. *Phys. Rev. Lett.* 121(5), 051101. <https://doi.org/10.1103/PhysRevLett.121.051101>. URL: <https://link.aps.org/doi/10.1103/PhysRevLett.121.051101>.
- Aguilar, M., Ali Cavazonza, L., Ambrosi, G., Arruda, L., Attig, N., Barao, F., Barrin, L., Bartoloni, A., Başeğmez-du Pree, S., Bates, J., Battiston, R., Behlmann, M., Beischer, B., Berdugo, J., Bertucci, B., Bindi, V., de Boer, W., Bollweg, K., Borgia, B., Boschini, M., Bourquin, M., Bueno, E., Burger, J., Burger, W., Burmeister, S., Cai, X., Capell, M., Casaus, J., Castellini, G., Cervelli, F., Chang, Y., Chen, G., Chen, H., Chen, Y., Cheng, L., Chou, H., Chouridou, S., Choutko, V., Chung, C., Clark, C., Coignet, G., Consolandi, C., Contin, A., Corti, C., Cui, Z., Dadzie, K., Dai, Y., Delgado, C., Della Torre, S., Demirköz, M., Derome, L., Di Falco, S., Di Felice, V., Díaz, C., Dimiccoli, F., von Doetinchem, P., Dong, F., Donnini, F., Duranti, M., Egorov, M., Egorov, A., Eline, A., Feng, J., Fiandrini, E., Fisher, P., Formato, V., Freeman, C., Galaktionov, Y., Gámez, C., García-López, R., Gargiulo, C., Gast, H., Gebauer, I., Gervasi, M., Giovacchini, F., Gómez-Coral, D., Gong, J., Goy, C., Grabski, V., Grandi, D., Graziani, M., Guo, K., Haino, S., Han, K., Hashmani, R., He, Z., Heber, B., Hsieh, T., Hu, J., Huang, Z., Hungerford, W., Incagli, M., Jang, W., Jia, Y., Jinch, H., Kanishev, K., Khiali, B., Kim, G., Kirn, T., Konyushikhin, M. et al., 2021. The Alpha Magnetic Spectrometer (AMS) on the international space station: Part II – Results from the first seven years. *Physics Reports*, 894, 1–116. <https://doi.org/10.1016/j.physrep.2020.09.003>, URL: <https://linkinghub.elsevier.com/retrieve/pii/S0370157320303434>.
- Aleksandrov, L., 1971. The newton-kantorovich regularized computing processes. *USSR Comput. Mathe. Mathe. Phys.* 11 (1), 46–57. [https://doi.org/10.1016/0041-5553\(71\)90098-X](https://doi.org/10.1016/0041-5553(71)90098-X).
- Aster, R., Borchers, B., Thurber, C., 2005. *Parameter Estimation and Inverse Problems*. Elsevier, New York.
- Bruno, A., Bazilevskaya, G.A., Boezio, M., Christian, E.R., Nolfo, G.A., d., Martucci, M., Merge', M., Mikhailov, V.V., Munini, R., Richardson, I.G., Ryan, J.M., Stochaj, S., Adriani, O., Barbarino, G.C., Bellotti, R., Bogomolov, E.A., Bongì, M., Bonvicini, V., Bottai, S., Cafagna, F., Campana, D., Carlson, P., Casolino, M., Castellini, G., Santis, C.D., Felice, V.D., Galper, A.M., Karelin, A.V., Koldashov, S. V., Koldobskiy, S., Krutkov, S.Y., Kvashnin, A.N., Leonov, A., Malakhov, V., Marcelli, L., Mayorov, A.G., Menn, W., Mocchiutti, E., Monaco, A., Mori, N., Osteria, G., Panico, B., Papini, P., Pearce, M., Picozza, P., Ricci, M., Ricciarini, S.B., Simon, M., Sparvoli, R., Spillantini, P., Stozhkov, Y.I., Vacchi, A., Vannuccini, E., Vasilyev, G. I., Voronov, S.A., Yurkin, Y.T., Zampa, G., Zampa, N., 2018. Solar Energetic Particle Events Observed by the PAMELA Mission. *Astrophys. J.*, 862(2), 97. <https://doi.org/10.3847/1538-4357/aacc26>, URL: <http://stacks.iop.org/0004-637X/862/i=2/a=97?key=crossref.45859fde94ef846644c45b84bc879c37>, <http://arxiv.org/abs/1807.10183%0Ahttps://doi.org/10.3847/1538-4357/aacc26>.
- Bütikofer, R., Flückiger, E., Desorgher, L., Moser, M., Pirard, B., 2009. The solar cosmic ray ground-level enhancements on 20 january 2005 and 13 december 2006. *Adv. Space Res.* 43 (4), 499–503.
- Caballero-Lopez, R., Moraal, H., 2012. Cosmic-ray yield and response functions in the atmosphere. *J. Geophys. Res.* 117, A12103.
- Cramp, J., Duldig, M., Flückiger, E., Humble, J., Shea, M., Smart, D., 1997. The october 22, 1989, solar cosmic enhancement: ray an analysis the anisotropy spectral characteristics. *J. Geophys. Res.* 102 (A11), 24 237–24 248.
- Ellison, D.C., Ramaty, R., 1985. Shock acceleration of electrons and ions in solar flares. *Astrophys. J.* 298, 400. <https://doi.org/10.1086/163623>, URL: http://articles.adsabs.harvard.edu/cgi-bin/nph-iarticle_query?1985ApJ...298.400E&data_type=PDF_HIGH&whole_paper=YES&type=PRINTER&filetype=.pdf, <http://adsabs.harvard.edu/cgi-bin/>

- nph-data_query?bibcode=1985ApJ...298.400E&link_type=ABSTRACT.
- Gil, A., Usoskin, I., Kovaltsov, G., Mishev, A., Corti, C., Bindi, V., 2015. Can we properly model the neutron monitor count rate? *J. Geophys. Res.* 120, 7172–7178.
- Gleeson, L.J., Axford, W.I., 1968. Solar Modulation of Galactic Cosmic Rays. *Astrophys. J.* 154, 1011. <https://doi.org/10.1086/149822>, URL: http://articles.adsabs.harvard.edu/cgi-bin/nph-article_query?1968ApJ...154.1011G&data_type=PDF_HIGH&whole_paper=YES&type=PRINTER&filetype=.pdf.
- Golub, G., Hansen, P., O'Leary, D.P., 1999. Tikhonov regularization and total least squares. *SIAM J. Matrix Anal. Appl.* 21, 185–194.
- Golub, G., Van Loan, C., 1980. An analysis of the total least squares problem. *SIAM J. Numer. Anal.* 17 (6), 883–893.
- Kocharov, L., Omodei, N., Mishev, A., Pesce-Rollins, M., Longo, F., Yu, S., Gary, D., Vainio, R., Usoskin, I., 2021. Multiple sources of solar high-energy protons. *Astrophys. J.* 915 (1). <https://doi.org/10.3847/1538-4357/abff57>.
- Kocharov, L., Pesce-Rollins, M., Laitinen, T., Mishev, A., Kühl, P., Klassen, A., Jin, M., Omodei, N., Longo, F., Webb, D., Cane, H., Heber, B., Vainio, R., Usoskin, I., 2020. Interplanetary protons versus interacting protons in the 2017 september 10 solar eruptive event. *Astrophys. J.* 890 (1). <https://doi.org/10.3847/1538-4357/ab684e>.
- Kocharov, L., Pohjolainen, S., Reiner, M., Mishev, A., Wang, H., Usoskin, I., Vainio, R., 2018. Spatial organization of seven extreme solar energetic particle events. *Astrophys. J. Lett.* 862 (2). <https://doi.org/10.3847/2041-8213/aad18d>.
- Koldobskiy, S., Raukunen, O., Vainio, R., Kovaltsov, G.A., Usoskin, I., 2021. New reconstruction of event-integrated spectra (spectral fluences) for major solar energetic particle events. *Astron. Astrophys.* 647, A132. <https://doi.org/10.1051/0004-6361/202040058>, URL: <https://www.aanda.org/10.1051/0004-6361/202040058>.
- Koldobskiy, S.A., Bindi, V., Corti, C., Kovaltsov, G.A., Usoskin, I.G., 2019a. Validation of the neutron monitor yield function using data from AMS-02 experiment, 2011–2017. *J. Geophys. Res.: Space Phys.* 124 (4), 2367–2379. <https://doi.org/10.1029/2018JA026340>, URL: <https://onlinelibrary.wiley.com/doi/abs/10.1029/2018JA026340>, <http://arxiv.org/abs/1904.01929>.
- Koldobskiy, S.A., Kovaltsov, G.A., Mishev, A.L., Usoskin, I.G., 2019b. New Method of Assessment of the Integral Fluence of Solar Energetic (> 1 GV Rigidity) Particles from Neutron Monitor Data. *Sol. Phys.* 294 (7), 94. <https://doi.org/10.1007/s11207-019-1485-8>, URL: <http://link.springer.com/10.1007/s11207-019-1485-8>.
- Koldobskiy, S.A., Kovaltsov, G.A., Usoskin, I.G., 2018. Effective Rigidity of a Polar Neutron Monitor for Recording Ground-Level Enhancements. *Sol. Phys.* 293 (7), 110. <https://doi.org/10.1007/s11207-018-1326-1>, URL: <http://link.springer.com/10.1007/s11207-018-1326-1>.
- Levenberg, K., 1944. A method for the solution of certain non-linear problems in least squares. *Q. Appl. Math.* 2, 164–168.
- Mangeard, P.-S., Ruffolo, D., Sáiz, A., Nuntiyakul, W., Bieber, J., Clem, J., Evenson, P., Pyle, R., Duldig, M., Humble, J., 2016. Dependence of the neutron monitor count rate and time delay distribution on the rigidity spectrum of primary cosmic rays. *J. Geophys. Res.: Space Phys.* 121 (12), 11620–11636. <https://doi.org/10.1002/2016JA023515>.
- Mangeard, P.-S., Ruffolo, D., Sáiz, A., Madlee, S., Nutaro, T., 2016. Monte carlo simulation of the neutron monitor yield function. *J. Geophys. Res. A: Space Phys.* 121 (8), 7435–7448. <https://doi.org/10.1002/2016JA022638>.
- Marquardt, D., 1963. An algorithm for least-squares estimation of nonlinear parameters. *SIAM J. Appl. Math.* 11 (2), 431–441.
- Mavrodiev, S., Mishev, A., Stamenov, J., 2004. A method for energy estimation and mass composition determination of primary cosmic rays at the chacaltaya observation level based on the atmospheric cherenkov light technique. *Nucl. Instrum. Methods Phys. Res., Section A: Accel., Spectrom., Detect. Associated Equip.* 530 (3), 359–366. <https://doi.org/10.1016/j.nima.2004.04.226>.
- Mavromichalaki, H., Gerontidou, M., Paschalidis, P., Paouris, E., Tezari, A., Sgouropoulos, C., Crosby, N., Dierckx, M., 2018. Real-time detection of the ground level enhancement on 10 september 2017 by a. ne.mo.s.: System report. *Space Weather* 16 (11), 1797–1805. <https://doi.org/10.1029/2018SW001992>.
- Mavromichalaki, H., Papaioannou, A., Plainaki, C., Sarlanis, C., Souvatzoglou, G., Gerontidou, M., Papailiou, M., Eroshenko, E., Belov, A., Yanke, V., Flückiger, E., Büttikofer, R., Parisi, M., Storini, M., Klein, K.-L., Fuller, N., Steigies, C., Rother, O., Heber, B., Wimmer-Schweingruber, R., Kudela, K., Strharsky, I., Langer, R., Usoskin, I., Ibragimov, A., Chilingaryan, A., Hovsepian, G., Reymers, A., Yeghikyan, A., Kryakunova, O., Dryn, E., Nikolayevskiy, N., Dorman, L., Pustil'Nik, L., 2011. Applications and usage of the real-time neutron monitor database. *Adv. Space Res.* 47, 2210–2222.
- McCracken, K., Rao, V., Shea, M., 1962. The Trajectories of Cosmic Rays in a High Degree Simulation of the Geomagnetic Field. Technical Report 77 Massachusetts Institute of Technology Cambridge, MA, USA.
- Mironova, I., Aplin, K., Arnold, F., Bazilevska, G., Harrison, R., Krivolutsky, A., Nicoll, K., Rozanov, E., Turunen, E., Usoskin, I., 2015. Energetic particle influence on the earth's atmosphere. *Space Science Rev.* 96.
- Miroshnichenko, L., 2018. Retrospective analysis of gles and estimates of radiation risks. *J. Space Weather Space Climate* 8, A52. <https://doi.org/10.1051/swsc/2018042>.
- Mishev, A., Poluianov, S., Usoskin, S., 2017. Assessment of spectral and angular characteristics of sub-gle events using the global neutron monitor network. *J. Space Weather Space Climate* 7, A28. <https://doi.org/10.1051/swsc/2017026>.
- Mishev, A., Usoskin, I., 2016a. Analysis of the ground level enhancements on 14 July 2000 and on 13 december 2006 using neutron monitor data. *Sol. Phys.* 291 (4), 1225–1239.
- Mishev, A., Usoskin, I., 2016b. Erratum to: analysis of the ground level enhancements on 14 July 2000 and on 13 december 2006 using neutron monitor data. *Sol. Phys.* 291 (4), 1579–1580.
- Mishev, A., Usoskin, I., 2018. Assessment of the radiation environment at commercial jet-flight altitudes during gle 72 on 10 September 2017 using neutron monitor data. *Space Weather* 16 (12), 1921–1929. <https://doi.org/10.1029/2018SW001946>.
- Mishev, A., Usoskin, I., 2020. Current status and possible extension of the global neutron monitor network. *J. Space Weather Space Clim* 10. <https://doi.org/10.1051/swsc/2020020>.
- Mishev, A., Usoskin, I., Kovaltsov, G., 2013. Neutron monitor yield function: New improved computations. *J. Geophys. Res.* 118, 2783–2788.
- Mishev, A., Usoskin, I., Raukunen, O., Paassilta, M., Valtonen, E., Kocharov, L., Vainio, R., 2018. First analysis of gle 72 event on 10 September 2017: Spectral and anisotropy characteristics. *Sol. Phys.* 293, 136.
- Mishev, A.L., Koldobskiy, S.A., Kocharov, L.G., Usoskin, I.G., 2021a. GLE # 67 Event on 2 November 2003: An Analysis of the Spectral and Anisotropy Characteristics Using Verified Yield Function and Detrended Neutron Monitor Data. *Sol. Phys.* 296 (5), 79. <https://doi.org/10.1007/s11207-021-01832-2>, URL: <https://doi.org/10.1007/s11207-021-01832-2>, <https://link.springer.com/10.1007/s11207-021-01832-2>.
- Mishev, A.L., Koldobskiy, S.A., Kovaltsov, G.A., Gil, A., Usoskin, I.G., 2020. Updated Neutron-Monitor Yield Function: Bridging Between In Situ and Ground-Based Cosmic Ray Measurements. *Journal of Geophysical Research: Space Physics* 125 (2). <https://doi.org/10.1029/2019JA027433>, URL: <https://onlinelibrary.wiley.com/doi/abs/10.1029/2019JA027433>.
- Mishev, A.L., Koldobskiy, S.A., Usoskin, I.G., Kocharov, L.G., Kovaltsov, G.A., 2021b. Application of the Verified Neutron Monitor Yield Function for an Extended Analysis of the GLE # 71 on 17 May 2012. *Space Weather* 19 (2). <https://doi.org/10.1029/2020SW002626>, URL: <https://onlinelibrary.wiley.com/doi/10.1029/2020SW002626>.
- Nuntiyakul, W., Sáiz, A., Ruffolo, D., Mangeard, P.-S., Evenson, P., Bieber, J., Clem, J., Pyle, R., Duldig, M., Humble, J., 2018. Bare

- neutron counter and neutron monitor response to cosmic rays during a 1995 latitude survey. *J. Geophys. Res.: Space Phys.* 123 (9), 7181–7195. <https://doi.org/10.1029/2017JA025135>.
- Poluianov, S.V., Usoskin, I.G., Mishev, A.L., Shea, M.A., Smart, D.F., 2017. GLE and Sub-GLE Redefinition in the Light of High-Altitude Polar Neutron Monitors. *Sol. Phys.* 292 (11), 176. <https://doi.org/10.1007/s11207-017-1202-4>.
- Potgieter, M., 2013. Solar Modulation of Cosmic Rays. *Living Rev. Sol. Phys.* 10 (1), 3. <https://doi.org/10.12942/lrsp-2013-3>, URL: <http://link.springer.com/10.12942/lrsp-2013-3>.
- Raukunen, O., Paassilta, M., Vainio, R., Rodriguez, J.V., Eronen, T., Crosby, N., Dierckxsens, M., Jiggins, P., Heynderickx, D., Sandberg, I., 2020. Very high energy proton peak flux model. *J. Space Weather Space Climate* 10, 24. <https://doi.org/10.1051/swsc/2020024>, URL: <https://www.swsc-journal.org/10.1051/swsc/2020024>.
- Shea, M., Smart, D., 1982. Possible evidence for a rigidity-dependent release of relativistic protons from the solar corona. *Space Sci. Rev.* 32, 251–271.
- Tikhonov, A., Goncharsky, A., Stepanov, V., Yagola, A., 1995. *Numerical Methods for Solving ill-Posed Problems*. Kluwer Academic Publishers, Dordrecht.
- Usoskin, I., Koldobskiy, S., Kovaltsov, G.A., Gil, A., Usoskina, I., Willamo, T., Ibragimov, A., 2020. Revised GLE database: Fluences of solar energetic particles as measured by the neutron-monitor network since 1956. *Astron. Astrophys.* 640, A17. <https://doi.org/10.1051/0004-6361/202038272>, URL: <https://www.aanda.org/10.1051/0004-6361/202038272>.
- Usoskin, I.G., 2017. A history of solar activity over millennia. *Living Rev. Sol. Phys.* 14 (1), 3. <https://doi.org/10.1007/s41116-017-0006-9>, URL: <http://link.springer.com/10.1007/s41116-017-0006-9>.
- Vainio, R., Desorgher, L., Heynderickx, D., Storini, M., Flückiger, E., Horne, R., Kovaltsov, G., Kudela, K., Laurenza, M., McKenna-Lawlor, S., Rothkaehl, H., Usoskin, I., 2009. Dynamics of the earth's particle radiation environment. *Space Sci. Rev.* 147 (3–4), 187–231.
- Vashenyuk, E., Balabin, Y., Gvozdevsky, B., Schur, L., 2008. Characteristics of relativistic solar cosmic rays during the event of december 13, 2006. *Geomag. Aeron.* 48 (2), 149–153.
- Vashenyuk, E., Balabin, Y., Perez-Peraza, J., Gallegos-Cruz, A., Miroshnichenko, L., 2006. Some features of the sources of relativistic particles at the sun in the solar cycles 21–23. *Adv. Space Res.* 38 (3), 411–417.